The ν_5 antisymmetric stretching mode of linear C_7 revisited in high resolution

J. Krieg,[a] V. Lutter, F.-X. Hardy, S. Schlemmer, and T. F. Giesen
I. Physikalisches Institut, Universität zu Köln, Zülpicher Str. 77, 50937 Köln, Germany

(Received 23 March 2010; accepted 29 April 2010; published online 8 June 2010)

The ν_5 antisymmetric stretching mode of the linear carbon cluster C_7 has been revisited using a sensitive high-resolution spectrometer, including an external-cavity quantum cascade laser covering the range of interest of 1894–1901 cm^{-1}. 50 transitions of the ν_5-band have been recorded and analyzed together with 45 transitions of the ν_4-band measured by Neubauer-Guenther *et al.* [J. Chem. Phys. **127**, 014313 (2007)]. We determined the band centers, rotational and centrifugal constants very precisely. In addition, 29 hot band transitions have been measured and tentatively assigned to the $\nu_5+\nu_{11}-\nu_{11}$ hot band. A global fit of the hot bands $\nu_5+\nu_{11}-\nu_{11}$ and $\nu_4+\nu_{11}-\nu_{11}$ is presented. Derived *l*-type doubling constants allow for an experimental estimation of the ν_{11}-band center. © *2010 American Institute of Physics*. [doi:10.1063/1.3431964]

I. INTRODUCTION

Pure carbon clusters, C_n, $n=2,3,4\ldots$, are believed to play an important role in the chemical processes of carbon-rich environments in space. Chemical network models of regions such as the envelopes of late type stars, e.g., IRC+10216, show pathways to carbonaceous species which undergo carbon enrichment and hydrogen depletion (see, e.g., Ref. 1). Understanding the formation process of pure carbon clusters and their detection in space are thus key to test and verify these models. So far, only C_2, C_3, and C_5 have been detected in diffuse clouds, shells of carbon stars, and in the interstellar medium via rovibronic or electronic spectroscopy (see Refs. 2–5). A systematic search for larger carbon clusters lacks experimental data in the mid-infrared (IR) and far-IR.

Of clusters known to exist, antisymmetric stretching vibrations of C_3 to C_{10} and C_{13} in the mid-IR region have been recorded by means of laboratory spectroscopy with resolved rotational structure, which allows for an unambiguous detection in space (e.g., Refs. 6–14). However, low-energy bending modes of these molecules are more relevant for astronomical purposes because these are more likely excited in cool environments where carbon chain molecules are formed. So far, the ν_2-band of C_3 is the only low lying bending vibration of all pure carbon chains which is known experimentally. To measure bending modes of other carbon chain molecules in high spectral resolution, a good prediction for the band center is needed. This may either come from high-level *ab initio* calculations or experimentally from high-resolution IR spectra of hot band transitions.

For a detailed analysis of the IR active stretching vibrations and associated hot bands of carbon clusters, tunable radiation sources with large spectral coverage in the region around 2000 cm^{-1} are needed. In our ongoing efforts to cover large portions of the mid-IR region with high-resolution lasers, a tunable external-cavity quantum cascade laser (EC-QCL) system has been implemented in our existing carbon cluster spectrometer to achieve a mode-hop free spectral coverage of about 50 cm^{-1} with this single laser.

We applied the new setup for a revision of the ν_5-band analysis of linear C_7. Our understanding of the properties of the linear carbon cluster C_7 has improved recently based on new high resolution laboratory data.[10] Measurements on the ν_4 fundamental band at 2138 cm^{-1} proved the molecule to be rather rigid, in agreement with high-level *ab initio* calculations performed by Botschwina.[15] This finding is in contrast to earlier results by Heath *et al.*,[16] who reported C_7 to be a very floppy molecule, indicated by large differences in the rotational constants of ground state and first excited ν_{11} bending state. To extend the set of accurate data on linear C_7, measurements on the ν_5 fundamental vibrational mode were performed and hot band transitions were measured for the first time, thanks to the improved sensitivity of the spectrometer.

In the present paper we report results from carbon cluster spectroscopy using a highly accurate, narrow linewidth quantum cascade laser system (Daylight Solutions, Ref. 17) to obtain very precise molecular data. The ν_5 fundamental band of C_7 has been recorded with a spectral accuracy of the order of 10^{-4} cm^{-1}. A simultaneous fit of these transition frequencies with data from the ν_4 fundamental band measured by Neubauer-Guenther *et al.*[10] was performed. Our analysis gives further proof for the rigidity of C_7. The characteristics and the performance of the EC-QCL system for spectroscopy of transient molecules, such as carbon clusters are discussed.

In addition, another band of a linear molecule has been detected. For these lines, we present strong arguments for their assignment to the hot band transition $\nu_5+\nu_{11}-\nu_{11}$ of the linear C_7 cluster involving the lowest bending mode ν_{11}.

[a]Electronic mail: krieg@ph1.uni-koeln.de.

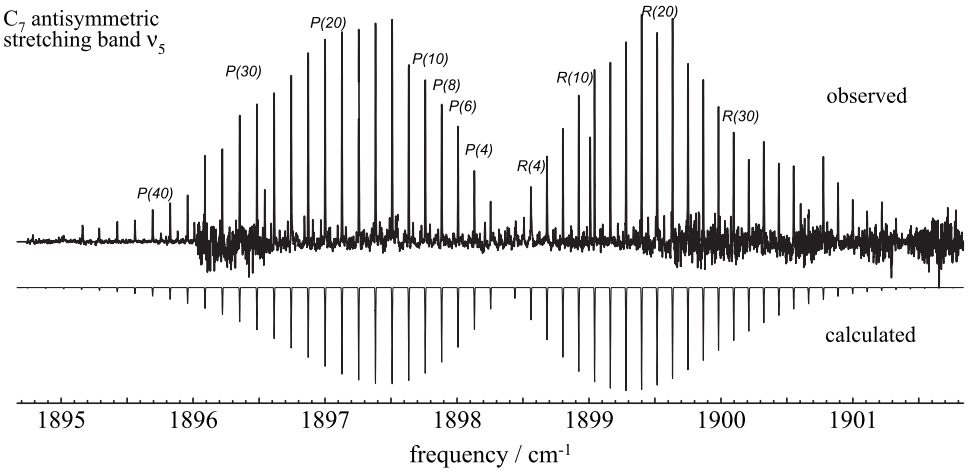

FIG. 1. The ν_5 fundamental band of linear C_7 at 1898 cm^{-1} and the calculated spectrum at T=25 K. Odd numbered transitions of J'' are missing due to spin statistics.

II. EXPERIMENT

A high resolution IR laser spectrometer covering the spectral range around 1900 cm^{-1} was used in combination with a laser ablation source for carbon cluster production (see Ref. 11). The latter consists of a pulsed UV laser focused onto a rotating graphite rod. A pulse of helium gas at backing pressures of around 15 bar carries the ablated carbon material through a slit source into a vacuum chamber. A set of roots pumps keeps the background pressure in the chamber below 0.05 mbar, where the gas is expanding adiabatically, forming a supersonic jet. Typically, rotational temperatures of 20 K are achieved with this setup. A high resolution IR laser beam passes the jet more than 40 times in a Herriott-type multipass optics. The transmitted laser intensity is recorded on a l-N_2 cooled HgCdTe-detector. For calibration purposes, the absorption spectra of a reference gas (N_2O) and fringes of a Fabry–Pérot étalon are simultaneously recorded. Significant improvements to the experimental setup were made to enhance the performance of the spectrometer in terms of sensitivity and frequency accuracy.

Instead of a tunable lead-salt diode laser, a high power mode-hop free tunable, continuous-wave EC-QCL system (*Daylight Solutions* Ref. 17) was used as IR radiation source. The system consists of a Quantum Cascade Laser which is locked to an external cavity. The technique and applications of EC-QCLs have been described, e.g., in Refs. 18–20. The system provides an optical output power of more than 30 mW and a complete spectral coverage of the range from 1875 to 1935 cm^{-1}. The laser linewidth is specified as less than 45 MHz. The small long term thermal frequency drift behavior allows for slow scans at high resolution over more than 40 GHz.

To improve calibration accuracy, we replaced the solid germanium étalon by a home-built internally coupled Fabry–Pérot interferometer (icFPI, Ref. 21), designed for high thermal stability. The étalon's free spectral range was 300 MHz. Because a frequency scan over 30 GHz takes up to one hour, thermal stability is important for reaching high calibration accuracies. We were able to increase the frequency accuracy by a factor of 2–5 compared to earlier measurements with the same spectrometer and a solid germanium étalon of 450 MHz free spectral range.

The strength of the absorption signal depends on the output power stability of the ablating laser. The frequency of a Q-switched Nd:YAG (yttrium aluminum garnet) laser is quadrupled to generate a wavelength of 266 nm at repetition rates of 20 Hz. Compared to the formerly used Excimer laser, the Nd:YAG laser allows for very stable jet conditions over many hours, which is crucial for extended frequency scans and for stable line intensity conditions.

III. RESULTS

We recorded 50 rovibrational transitions in the spectral range between 1895 and 1901.5 cm^{-1} and assigned them to the $P(48)$ to $R(50)$ transitions of the ν_5 fundamental band of C_7. Observed frequencies are listed in Table I. C_7 is a centrosymmetric molecule of point group symmetry $D_{\infty h}$ which has a Σ_g^+ electronic ground state. Due to nuclear spin statistics of carbon, there are no energy levels with even-numbered rotational quantum numbers J in the ground state. This results in a frequency spacing of neighboring lines of roughly four times the rotational constant B.

The experimental spectrum is shown in the upper part of Fig. 1, and a calculated spectrum based on a least-squares fit of molecular parameters is plotted below. The measurements comprise 32 separate frequency scans ranging from 0.2 to 1.2 cm^{-1}. Overlapping spectra have been averaged with a binning of 5×10^{-4} cm^{-1}. Regions of weak lines have been scanned several times and spectra have been co-added for better signal-to-noise ratios. As an example for a single scan spectrum the $R(24)$ transition is depicted in Fig. 2. The line intensity distribution of P- and R-branch transitions is best reproduced by a Boltzmann distribution at a rotational temperature of 25 K.

The observed linewidths of about 120 MHz full width at half maximum (FWHM) are due to Doppler broadening caused by the velocity component of the molecular jet along the line of sight. Linewidths of 120 MHz correspond to a molecular velocity dispersion of roughly ±300 m/s along the

TABLE I. Measured transition frequencies of the ν_5 fundamental of C_7 in cm^{-1}. Best fit residuals are also given.

J	$R(J)$	Obs.-Calc. ($\times 10^{-3}$)	$P(J)$	Obs.-Calc. ($\times 10^{-3}$)
0	1898.4406	1.9	…	…
2	1898.5608	0.2	1898.2547	−0.3
4	1898.6813	−0.6	1898.1314	−0.5
6	1898.8027	0.0	1898.0077	−0.5
8	1898.9228	−0.1	1897.8838	−0.2
10	1899.0424	−0.3	1897.7597	0.4
12	1899.1612	−0.7	1897.6341	0.0
14	1899.2805	−0.1	1897.5083	−0.0
16	1899.3990	0.2	1897.3819	−0.1
18	1899.5164	−0.1	1897.2548	−0.5
20	1899.6337	0.1	1897.1280	0.1
22	1899.7509	0.7	1897.0001	0.0
24	1899.8666	0.3	1896.8722	0.5
26	1899.9820	0.1	1896.7430	0.2
28	1900.0965	−0.4	1896.6137	0.3
30	1900.2114	−0.0	1896.4842	0.7
32	1900.3248	−0.6	1896.3537	0.6
34	1900.4390	0.1	1896.2217	−0.4
36	1900.5512	−0.7	1896.0902	−0.4
38	1900.6642	−0.1	1895.9575	−1.1
40	1900.7766	0.4	1895.8266	0.6
42	1900.8878	0.2	1895.6937	0.7
44	1900.9996	1.1	1895.5597	0.3
46	1901.1083	−0.6	1895.4257	0.4
48	1901.2198	1.1	1895.2893	−1.4
50	1901.3275	−0.5	…	…

line of sight, which is plausible for a slightly divergent jet when probed perpendicular. The linewidth of the laser is significantly smaller, since the étalon fringes of the calibration icFPI have a width of roughly 70 MHz (FWHM), see Fig. 3. The calculated finesse of 6, see Ref. 21, corresponds to fringes of about 50 MHz width, and thus the laser linewidth is certainly less than 70 MHz.

The achieved sensitivity of the spectrometer is better than $\Delta I/I = 1 \times 10^{-4}$, when averaging each spectral point over 30 shots of the pulsed molecular beam. We estimate the intensity of the ν_5-band to be five to ten times weaker than the ν_4-band, though a careful comparison is difficult due to different setups used to record the two bands.

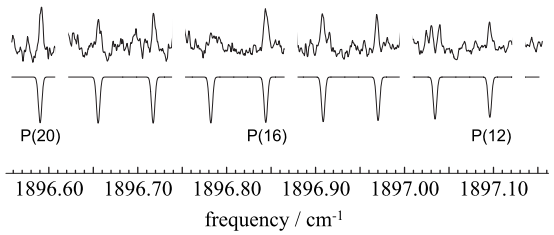

FIG. 2. Hot band transitions of C_7 at 1897 cm^{-1}. The strong ν_5 fundamental band transitions have been blanked out for better visibility of the weak hot band transitions. The lower trace shows a calculated spectrum of the $\nu_5+\nu_{11}-\nu_{11}$ hot band.

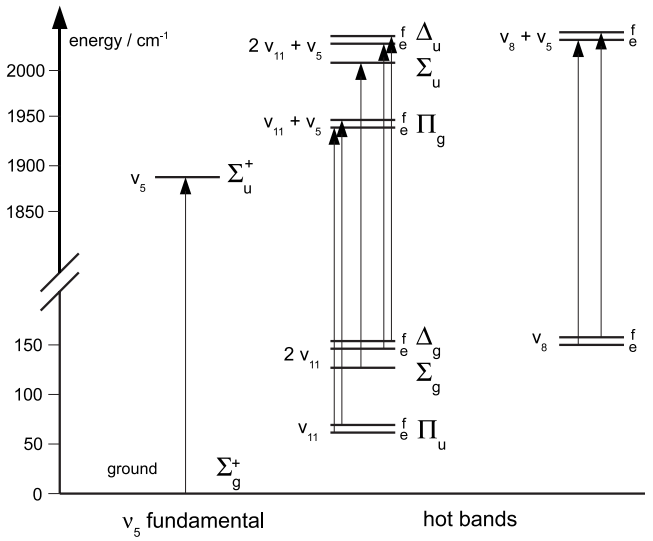

FIG. 3. Schematic energy level diagram for vibrational states of C_7. The two lowest ν_8 and ν_{11} bending energies are calculated to be 70 and 156 cm^{-1} (Ref. 15). For states in which the bending mode is excited, vibrational angular momentum has to be taken into account. l-type interaction splits $l>0$ states into two components with e and f symmetry. A similar scheme for the ν_4 vibration of linear C_7 is given in Ref. 10.

IV. ANALYSIS

A. The ν_5 fundamental band

In order to increase the accuracy of the determined ground state parameters, a global fit of the 50 observed

TABLE II. Measured transitions of the $\nu_5+\nu_{11}-\nu_{11}$ hot band of C_7 in cm^{-1}. Best fit residuals are also given. Values in parentheses are calculated upon best fit parameters, when unambiguous identification was not possible, e.g., due to blending with strong fundamental lines.

J	$R(J)$	Obs.-Calc. ($\times 10^{-3}$)	$P(J)$	Obs.-Calc. ($\times 10^{-3}$)
10	1898.5078	−0.3	(1897.2213)	…
11	1898.5674	0.5	1897.1584	−1.3
12	(1898.6279)	⋯	1897.0956	−0.4
13	(1898.6863)	⋯	1897.0331	−1.2
14	1898.7465	−0.7	1896.9689	−1.3
15	(1898.8052)	⋯	1896.9081	−0.4
16	1898.8670	0.9	1896.8441	0.1
17	(1898.9237)	⋯	1896.7861	3.9
18	1898.9842	−0.3	1896.7181	0.8
19	(1899.0416)	⋯	1896.6558	0.3
20	1899.1045	2.0	1896.5914	1.2
21	(1899.1591)	⋯	1896.5280	−0.2
22	1899.2191	−0.8	(1896.4625)	⋯
23	1899.2752	−1.0	(1896.4005)	⋯
24	1899.3379	1.0	(1896.3344)	⋯
25	(1899.3927)	⋯	(1896.2723)	⋯
26	1899.4506	−2.8	(1896.2058)	⋯
27	1899.5067	−2.1	(1896.1436)	⋯
28	1899.5705	1.0	(1896.0768)	⋯
29	1899.6251	0.7	(1896.0145)	⋯
30	1899.6855	0.5	1895.9475	0.3
31	(1899.7395)	⋯	1895.8833	−1.6
32	(1899.8001)	⋯	1895.8163	−0.9
33	(1899.8542)	⋯	1895.7570	2.2

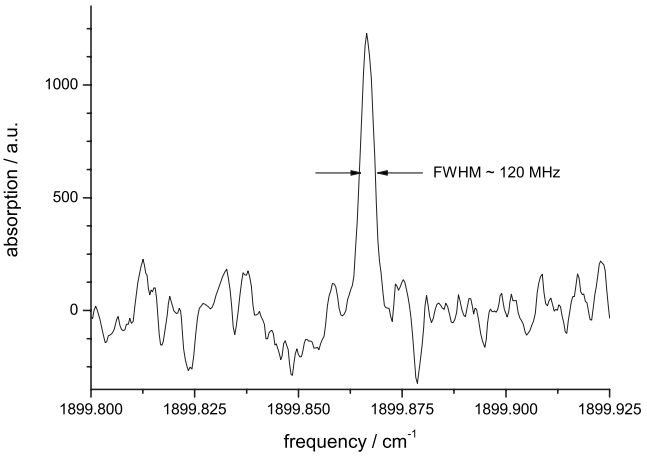

FIG. 4. $R(24)$ transition of the ν_5-band of C_7 with a linewidth (FWHM) of 120 MHz measured with a single scan.

ν_5-band transition frequencies together with 45 lines of the ν_4 fundamental band, taken from Ref. 10, was performed. The higher frequency accuracy of ν_5-band data compared to ν_4-band data was taken into account by weighting the ν_5-band transitions with a factor of 2. The open source program PGOPHER was used for data analysis.[22] The unweighted average error of all fitted transitions was less than 35 and 20 MHz when only the new measurements of ν_5-band transitions were taken into account.

We have determined the ν_5-band origin unambiguously and with high accuracy to be 1898.377 61(11) cm^{-1}. This value is in good agreement with a band center position of 1898.3758(8) cm^{-1} published by Heath *et al.*,[23] although it is slightly above the 1σ error limit. It is worth mentioning that Heath *et al.* had not recorded the ν_5-band origin due to lack of appropriate diode lasers. Table III summarizes the molecular parameters obtained in this work, the parameters from Ref. 23 and the results from *ab initio* calculations by Botschwina.[15]

B. Hot band transitions

In addition to the ν_5 fundamental band, we detected lines from at least one other band of C_7. The upper part of Fig. 4 shows details of the recorded spectrum. For better visibility of weak transitions, fundamental band transitions have been blanked out. The observed lines of the hot band are listed in Table II. The spacing of adjacent lines is roughly two times the rotational constant B with a small alternation.

This so-called "staggering" is an indication for hot band transitions of a bending mode with vibrational angular momentum $l=1$. See Fig. 5 for an energy term scheme of C_7. ν_8 and ν_{11} are energetically low lying bending modes which could give rise to the observed hot band. Due to the low temperatures in the jet, we assume the hot band to be the $\nu_5+\nu_{11}-\nu_{11}$ vibration, because the lowest bending mode should be most populated besides the ground state.

The signal-to-noise ratio of these hot band transitions is small. In spite of averaging over many scans, these bands are not clearly visible over the whole recorded spectral range, which makes a secure assignment of lines hardly feasible. In particular, the band origin is not clearly determined. However, the molecular parameters for the bending mode ν_{11} are known with good accuracy from the hot band analysis of $\nu_4+\nu_{11}-\nu_{11}$ by Neubauer-Guenther *et al.* Using these parameters, the hot band $\nu_5+\nu_{11}-\nu_{11}$ has been assigned as shown in Fig. 4, when residuals of a least-squares fit are smallest.

Furthermore the data from Ref. 10 have been used for a global fit of ν_{11} hot band data. Results are given in Table IV.

TABLE III. Molecular parameters in cm^{-1} for ground state, and vibrational excited ν_4 and ν_5 states. α values from experimental data have been calculated from $B_i=B_e-\alpha_i(v_i+1/2)$. Line positions of the ν_4-band were taken from Ref. 10. The unweighted averaged error for our global fit was 0.000 72 cm^{-1}.

Parameter	Global fit (this work)	Neubauer-Guenther *et al.*[a]	Heath *et al.*[b]	*Ab initio*[c]
B_0	0.030 622 1(12)	0.030 624 4(28)	0.030 613(14)	0.030 63[d]
$D_0[\times 10^{-8}]$	<0.1[e]	…	−2.33(85)	0.0337[f]
$H_0[\times 10^{-12}]$	…	…	−5.4(15)	…
ν_4	2138.314 54(22)	2138.314 42(20)	2138.3152(5)	2203.8
$\alpha_4[\times 10^{-4}]$	1.157(16)	1.153(39)	1.17(20)	1.137
B_4	0.0305 064(11)	0.0305 091(27)	0.0304 96(14)	0.030 52[d]
$D_4[\times 10^{-8}]$	<0.1 [e]	…	−2.51(91)	…
$H_4[\times 10^{-12}]$	…	…	−5.9(17)	…
ν_5	1898.377 61(11)	…	1898.3758(8)	1933.3
$\alpha_5[\times 10^{-4}]$	0.653(16)	…	0.57(21)	0.6727
B_5	0.0305 568(11)	…	0.030 556(15)	0.030 57[d]
$D_5[\times 10^{-8}]$	0.152(43)	…	−1.6(11)	…
$H_5[\times 10^{-12}]$	…	…	−4.4(31)	…

[a]Reference 10.
[b]Reference 23.
[c]Reference 15.
[d]Calculated from B_e and α_i values as given in the reference.
[e]Including the given parameter does not improve the fit significantly. The 1σ deviation is given as an upper limit.
[f]*Ab initio* value for D_e as given in Ref. 15.

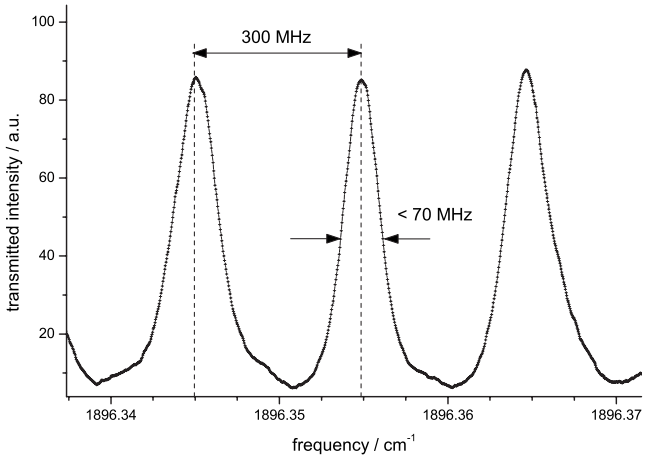

FIG. 5. Étalon fringes of an internally coupled Fabry–Pérot Interferometer. The finesse of $F^{\star} \approx 4.3$ is close to the expected theoretical value of 6 (see Ref. 21).

The average residual is 1.1×10^{-3} cm^{-1}, which is plausible for weak lines with less signal-to-noise ratio.

V. DISCUSSION

Compared to Ref. 23, the molecular parameters derived here are a factor of 5–10 more accurate. We attribute this to the improved calibration procedure involving the icFPI as étalon and the better signal-to-noise ratio. The set of molecular parameters required to reproduce the measured lines within error bars has been reduced to the band origins, the rotational constants B_4, B_5, and B_0 for the excited states in the ν_4- and ν_5-band and for the vibrational ground state, respectively. Only the D_5 centrifugal distortion parameter was found to be significant in the fit.

In contrast, the analysis presented in Ref. 23 leads to large and negative distortion constants for both the ground state and the excited state, which was attributed to an unknown perturbation. However, the 1σ error from our fit gives an estimation of the upper limits of D_4, which is two orders of magnitude smaller compared to Ref. 23. The simple Kratzer relation $D=4B^3/\omega^2$ points to rather small centrifugal distortion constants of $D_5 \approx 3 \times 10^{-11}$ cm^{-1}, which is in good agreement with our experimental results. Higher order distortion constants were not significant in the fit. Therefore, we conclude that both the ground state and the ν_5 excited state are not perturbed and that C_7 is surely a rigid molecule.

Our analysis is consistent with high-level *ab initio* calculations reported by Botschwina (Ref. 15). Table III lists these values as well, revealing a deviation of the calculated rotational constants of less than 0.05% from the experimental results. There are no calculated values for the distortion constants in the vibrational ground state and excited states, but the value of D_e in the equilibrium state is given, which is one order of magnitude smaller than our measured value and thus below the detection limit.

The band intensity of the ν_5-band transition is estimated to be five to ten times weaker than ν_4-band intensity, though a comparison is difficult because the two measurements were performed with different setups. The sensitivity of the spectrometer is on a level which allowed hot band transitions involving the ν_5-band to be detected for the first time. These are typically 10–20 times weaker than fundamental transitions.

TABLE IV. Parameters for the $\nu_4+\nu_{11}-\nu_{11}$ and $\nu_5+\nu_{11}-\nu_{11}$ hot bands are given in cm^{-1}. Line positions of the $\nu_4+\nu_{11}-\nu_{11}$ hot band were taken from Ref. 10. The average on the residuals was 0.0011 cm^{-1} and did not differ very much in the two bands.

Parameter	Global fit (this work)	Neubauer-Guenther *et al.*[a]	*Ab initio*[b]
B_{11}	0.030 674 4(37)	0.030 675 9(38)	0.030 78[c]
$q_{11}[\times 10^{-5}]$	4.54(74)	3.71(76)	2.68
$\nu_4+\nu_{11}-\nu_{11}$	2137.738 50(24)	2137.738 56(16)	⋯
B_{4+11}	0.030 560 7(40)	0.030 552 2(41)	0.030 61[c]
$q_{4+11}[\times 10^{-8}]$	4.62(78)	⋯	⋯
$\nu_5+\nu_{11}-\nu_{11}$	1898.840 53(40)	⋯	⋯
B_{5+11}	0.030 615 1(37)	⋯	0.030 68[c]
$q_{5+11}[\times 10^{-5}]$	4.56(74)	⋯	⋯

[a]Reference 10.
[b]Reference 15.
[c]Calculated from B_e and α_i values as given in the reference.

The presented tentative assignment of lines to the $\nu_5+\nu_{11}-\nu_{11}$ hot band is based on the analysis of Neubauer-Guenther *et al.* and the extended data set of the $\nu_4+\nu_{11}-\nu_{11}$ band. The frequency accuracy for these latter lines is about 50% less than for the fundamental transitions, which can be explained by the poor signal-to-noise level. The q parameter obtained here allows to estimate the band center of the bending mode ν_{11}. The approximation $\nu=f_q B_{11}^2/q$ yields a value of $\nu_{11}=44.6(73)$ cm^{-1} compared to $\nu_{11}=54(11)$ cm^{-1} taken from Ref. 10. Here, a value of $f_q=2.15(5)$ which was derived for C_3S_2 was used as explained in Ref. 10. It proved to be reasonable also for C_5 and C_9 (Refs. 8 and 12).

The new value for the ν_{11}-band center does not agree with the value calculated by Botschwina ($\nu_{11}=70$ cm^{-1}). The deviation is significant, but one has to consider that deriving band origins from l-type doubling constants gets more difficult for larger carbon chains. E.g., for C_9, the l-type doubling constant q is too small to be detected. A better signal-to-noise ratio could secure our assignment and analysis of the observed hot band.

The results with the improved Cologne Carbon Cluster Experiment show the high performance of the new setup. The frequency accuracy is now obviously on a very high level compared to similar setups and of the order of 10^{-4} cm^{-1}. The EC-QCL system is well suited for high resolution measurements offering high output power, small linewidth and large tuning range. In-house built EC-QCL systems (Ref. 20) promise similar performance for absorption spectroscopy and allow the option of changing the laser chip to further increase the spectral coverage with one system. These new radiation sources promise extension of extremely precise measurements to other carbon clusters as well.

ACKNOWLEDGMENTS

The authors thank the DFG for funding through Grant No. GI319/1-3 as part of the European project "Laboratoire Européen Associé—High Resolution Molecular Spectros-

copy" (LEA Hi-Res), and Mr. Godejohann from MG Optical Solutions GmbH for technical support.

[1] T. J. Millar, E. Herbst, and R. P. A. Bettens, Mon. Not. R. Astron. Soc. **316**, 195 (2000).
[2] D. Crampton, A. P. Cowley, and R. M. Humphreys, Astrophys. J. **198**, L135 (1975).
[3] T. F. Giesen, A. O. Van Orden, J. D. Cruzan, R. A. Provencal, R. J. Saykally, R. Gendriesch, F. Lewen, and G. Winnewisser, Astrophys. J. **551**, L181 (2001).
[4] J. P. Maier, N. M. Lakin, G. A. H. Walker, and D. A. Bohlender, Astrophys. J. **553**, 267 (2001).
[5] P. F. Bernath, K. H. Hinkle, and J. J. Keady, Science **244**, 562 (1989).
[6] K. Matsumura, H. Kanamori, and K. Kawaguchi, J. Chem. Phys. **89**, 3491 (1988).
[7] N. Moazzen-Ahmadi, J. J. Thong, and A. R. W. McKellar, J. Chem. Phys. **100**, 4033 (1994).
[8] N. Moazzen-Ahmadi, J. J. Thong, and A. R. W. McKellar, J. Chem. Phys. **91**, 2140 (1989).
[9] H. J. Hwang, A. Van Orden, K. Tanaka, E. W. Kuo, J. R. Heath, and R. J. Saykally, Mol. Phys. **79**, 769 (1993).
[10] P. Neubauer-Guenther, K. M. T. Yamada, T. F. Giesen, and S. Schlemmer, J. Chem. Phys. **127**, 014313 (2007).
[11] P. Neubauer-Guenther, T. F. Giesen, U. Berndt, G. Fuchs, and G. Winnewisser, Spectrochim. Acta, Part A **59**, 431 (2003).
[12] A. Van Orden, R. A. Provencal, F. N. Keutsch, and R. J. Saykally, J. Chem. Phys. **105**, 6111 (1996).
[13] T. F. Giesen, U. Berndt, K. M. T. Yamada, G. Fuchs, R. Schieder, G. Winnewisser, R. A. Provencal, F. N. Keutsch, A. Van Orden, and R. J. Saykally, ChemPhysChem **2**, 242 (2001).
[14] T. F. Giesen, A. Van Orden, H. J. Hwang, R. S. Fellers, R. A. Provencal, and R. J. Saykally, Science **265**, 756 (1994).
[15] P. Botschwina, Chem. Phys. Lett. **354**, 148 (2002).
[16] J. R. Heath and R. J. Saykally, J. Chem. Phys. **94**, 1724 (1991).
[17] Homepage of Daylight Solutions, http://daylightsolutions.com.
[18] G. Wysocki, R. F. Curl, F. K. Tittel, R. Maulini, J. M. Bulliard, and J. Faist, Appl. Phys. B: Lasers Opt. **81**, 769 (2005).
[19] G. Wysocki, R. Lewicky, R. F. Curl, F. K. Tittel, L. Diehl, F. Capasso, M. Troccoli, G. Hofler, D. Bour, S. Corzine, R. Maulini, M. Giovannini, and J. Faist, Appl. Phys. B: Lasers Opt. **92**, 305 (2008).
[20] D. Stupar, J. Krieg, P. Kroetz, G. Sonnabend, M. Sornig, T. F. Giesen, and R. Schieder, Appl. Opt. **47**, 2993 (2008).
[21] M. Reich, R. Schieder, H. J. Clar, and G. Winnewisser, Appl. Opt. **25**, 130 (1986).
[22] C. M. Western, PGOPHER, a program for simulating rotational structure. http://pgopher.chm.bris.ac.uk, 2008.
[23] J. R. Heath, A. Van Orden, E. Kuo, and R. J. Saykally, Chem. Phys. Lett. **182**, 17 (1991).